

Appendix A: Planetary parameters

Table A.1. Planetary parameters, validation status and FAP values for the first half of our candidates.

Parameters	TOI-1883.01	TOI-2274.01	TOI-2603.01	TOI-2768.01	TOI-2781.01	TOI-4438.01	TOI-5205.01
Validation status	Yes	Yes	No	Yes	Suggestive	Yes	No
R_p [R_\oplus]	$5.65^{+0.24}_{-0.24}$	$2.45^{+0.23}_{-0.13}$	$9.46^{+0.62}_{-0.59} / 11.55^{+2.29}_{-1.43}$	$2.63^{+0.45}_{-0.44}$	$6.20^{+0.42}_{-0.42} / 7.00^{+2.32}_{-0.80}$	$2.49^{+0.13}_{-0.13}$	$10.44^{+0.38}_{-0.38} / 11.24^{+0.88}_{-0.63}$
k_{app}	$0.1057^{+0.0013}_{-0.0012}$	$0.0350^{+0.0019}_{-0.0007}$	$0.1460^{+0.0042}_{-0.0037}$	$0.0367^{+0.0023}_{-0.0023}$	$0.0815^{+0.0031}_{-0.0032}$	$0.0606^{+0.0015}_{-0.0016}$	$0.2404^{+0.0027}_{-0.0027}$
k_{true}	$0.1076^{+0.0042}_{-0.0016}$	$0.0360^{+0.0021}_{-0.0007}$	$0.1782^{+0.0288}_{-0.0155}$	$0.0434^{+0.0130}_{-0.0050}$	$0.0907^{+0.0242}_{-0.0071}$	$0.0643^{+0.0052}_{-0.0022}$	$0.2590^{+0.0139}_{-0.0081}$
P_{orb} [days]	$4.50638^{+0.000007}_{-0.000006}$	$2.67963^{+0.000003}_{-0.000003}$	$1.332641^{+0.000002}_{-0.000002}$	$1.50801^{+0.000006}_{-0.000006}$	$2.76370^{+0.000008}_{-0.000008}$	$7.44630^{+0.000008}_{-0.000009}$	$1.63075^{+0.000002}_{-0.000002}$
a/R_*	$19.11^{+0.39}_{-0.87}$	$16.91^{+2.08}_{-2.25}$	$6.76^{+0.51}_{-0.41}$	$8.83^{+0.61}_{-1.50}$	$12.70^{+2.73}_{-1.79}$	$29.22^{+0.87}_{-2.14}$	$10.78^{+0.49}_{-0.40}$
a [AU]	$0.0468^{+0.0010}_{-0.0021}$	$0.050^{+0.0061}_{-0.0066}$	$0.0186^{+0.0014}_{-0.0011}$	$0.0270^{+0.0019}_{-0.0046}$	$0.0412^{+0.0089}_{-0.0058}$	$0.0511^{+0.0015}_{-0.0037}$	$0.02^{+0.0009}_{-0.0008}$
b	$0.21^{+0.15}_{-0.14}$	$0.78^{+0.63}_{-0.71}$	$0.43^{+0.10}_{-0.19}$	$0.34^{+0.30}_{-0.24}$	$0.64^{+0.11}_{-0.30}$	$0.25^{+0.19}_{-0.18}$	$0.38^{+0.08}_{-0.13}$
i [deg]	$89.37^{+0.42}_{-0.51}$	$87.37^{+0.50}_{-0.65}$	$86.33^{+1.82}_{-1.17}$	$87.78^{+1.57}_{-2.79}$	$86.33^{+1.82}_{-1.17}$	$89.51^{+0.36}_{-0.44}$	$87.98^{+0.49}_{-0.74}$
T_c [BJD]	$2459256.8481^{+0.0002}_{-0.0002}$	$2458685.3661^{+0.0009}_{-0.0009}$	$2459255.8235^{+0.0004}_{-0.0004}$	$2459225.6442^{+0.0010}_{-0.0011}$	$2459226.4327^{+0.0008}_{-0.0009}$	$2459396.4107^{+0.0006}_{-0.0006}$	$2459443.4714^{+0.0002}_{-0.0002}$
T_{eq} [K]	524.92	771.46	953.97	855	673	435±15	737±15
FAP (%)	0.00067	0.00067	>50	0.00067	17.2627	0.00067	>50

Table A.2. Planetary parameters, validation status and FAP values for the second half of our candidates.

Parameters	TOI-5268.01	TOI-5319.01	TOI-5344.01	TOI-5464.01	TOI-5486.01	TOI-5641.01
Validation status	No	Yes	No	No	Suggestive	No
R_p [R_\oplus]	$9.35^{+1.70}_{-1.82} / 10.79^{+3.27}_{-2.38}$	$2.83^{+0.57}_{-0.59}$	$10.47^{+0.47}_{-0.48} / 10.74^{+1.73}_{-0.59}$	$9.73^{+0.53}_{-0.55} / 10.11^{+0.74}_{-0.60}$	$3.14^{+0.49}_{-0.51} / 4.68^{+1.87}_{-0.83}$	$8.75^{+0.50}_{-0.48} / 8.99^{+0.96}_{-0.59}$
k_{app}	$0.2792^{+0.0418}_{-0.0452}$	$0.0536^{+0.0030}_{-0.0035}$	$0.1646^{+0.0017}_{-0.0019}$	$0.1693^{+0.0028}_{-0.0031}$	$0.0524^{+0.0067}_{-0.070}$	$0.1684^{+0.0025}_{-0.0021}$
k_{true}	$0.3222^{+0.0872}_{-0.0606}$	$0.0609^{+0.0092}_{-0.0035}$	$0.1689^{+0.0215}_{-0.0035}$	$0.1759^{+0.0061}_{-0.0038}$	$0.0694^{+0.0122}_{-0.0051}$	$0.1731^{+0.0113}_{-0.0041}$
P_{orb} [days]	$2.06859^{+0.000002}_{-0.000002}$	$4.07853^{+0.000008}_{-0.000008}$	$3.79262^{+0.000007}_{-0.000006}$	$1.16065^{+0.000004}_{-0.000004}$	$2.02470^{+0.000006}_{-0.000006}$	$2.18168^{+0.000008}_{-0.000008}$
a/R_*	$13.45^{+1.95}_{-0.76}$	$22.46^{+1.08}_{-2.66}$	$15.58^{+0.89}_{-0.46}$	$7.87^{+0.14}_{-0.24}$	$10.31^{+0.51}_{-1.45}$	$12.84^{+0.34}_{-0.63}$
a [AU]	$0.0192^{+0.0028}_{-0.0011}$	$0.0506^{+0.0025}_{-0.0060}$	$0.0422^{+0.0024}_{-0.0012}$	$0.0193^{+0.0003}_{-0.0006}$	$0.0264^{+0.0013}_{-0.0037}$	$0.0377^{+0.0010}_{-0.0018}$
b	$0.90^{+0.07}_{-0.10}$	$0.30^{+0.25}_{-0.20}$	$0.70^{+0.02}_{-0.05}$	$0.14^{+0.14}_{-0.10}$	$0.30^{+0.28}_{-0.22}$	$0.24^{+0.15}_{-0.15}$
i [deg]	$86.20^{+0.66}_{-0.47}$	$89.25^{+0.53}_{-0.82}$	$87.43^{+0.30}_{-0.16}$	$88.95^{+0.74}_{-1.09}$	$88.31^{+1.22}_{-2.06}$	$88.94^{+0.69}_{-0.73}$
T_c [BJD]	$2459661.6373^{+0.0004}_{-0.0004}$	$2459496.5862^{+0.0007}_{-0.0007}$	$2459522.8248^{+0.0007}_{-0.0007}$	$2459635.5575^{+0.0009}_{-0.0010}$	$2459691.0601^{+0.0006}_{-0.0006}$	$2459663.4852^{+0.0013}_{-0.0013}$
T_{eq} [K]	438	695	689±12	884	647	435±15
FAP (%)	>50	0.00067	>50	>50	2.9113	>50

Appendix B: Individual light curves and contamination analysis

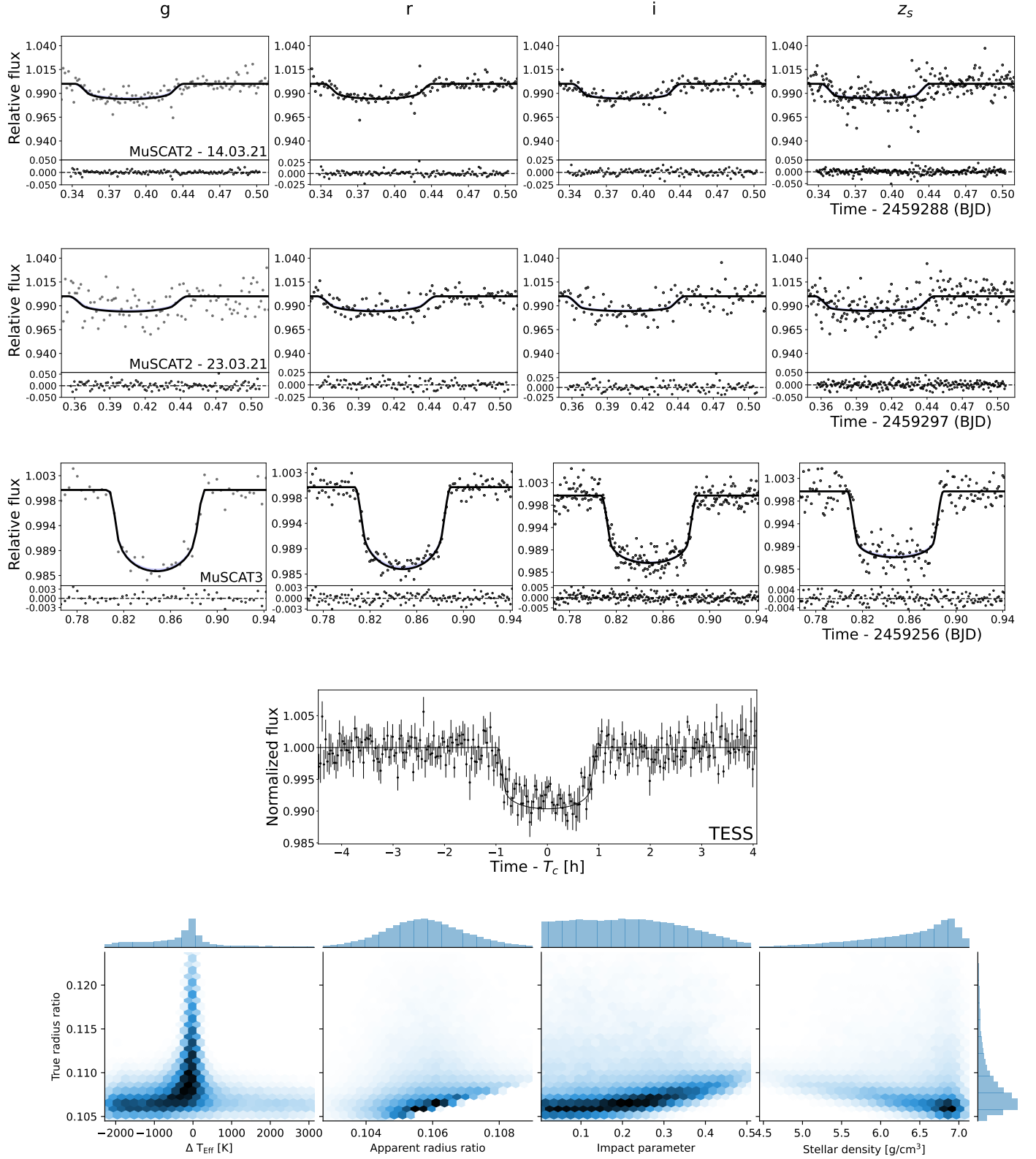


Fig. B.1. Top: TOI-1883b’s MuSCAT2 and TESS light-curves. Bottom: Contamination plot. Here we present the relation between the true radius ratio and the increase in effective temperature, the apparent radius, the impact parameter and the stellar density. As previously mentioned, the X axis may vary in between targets.

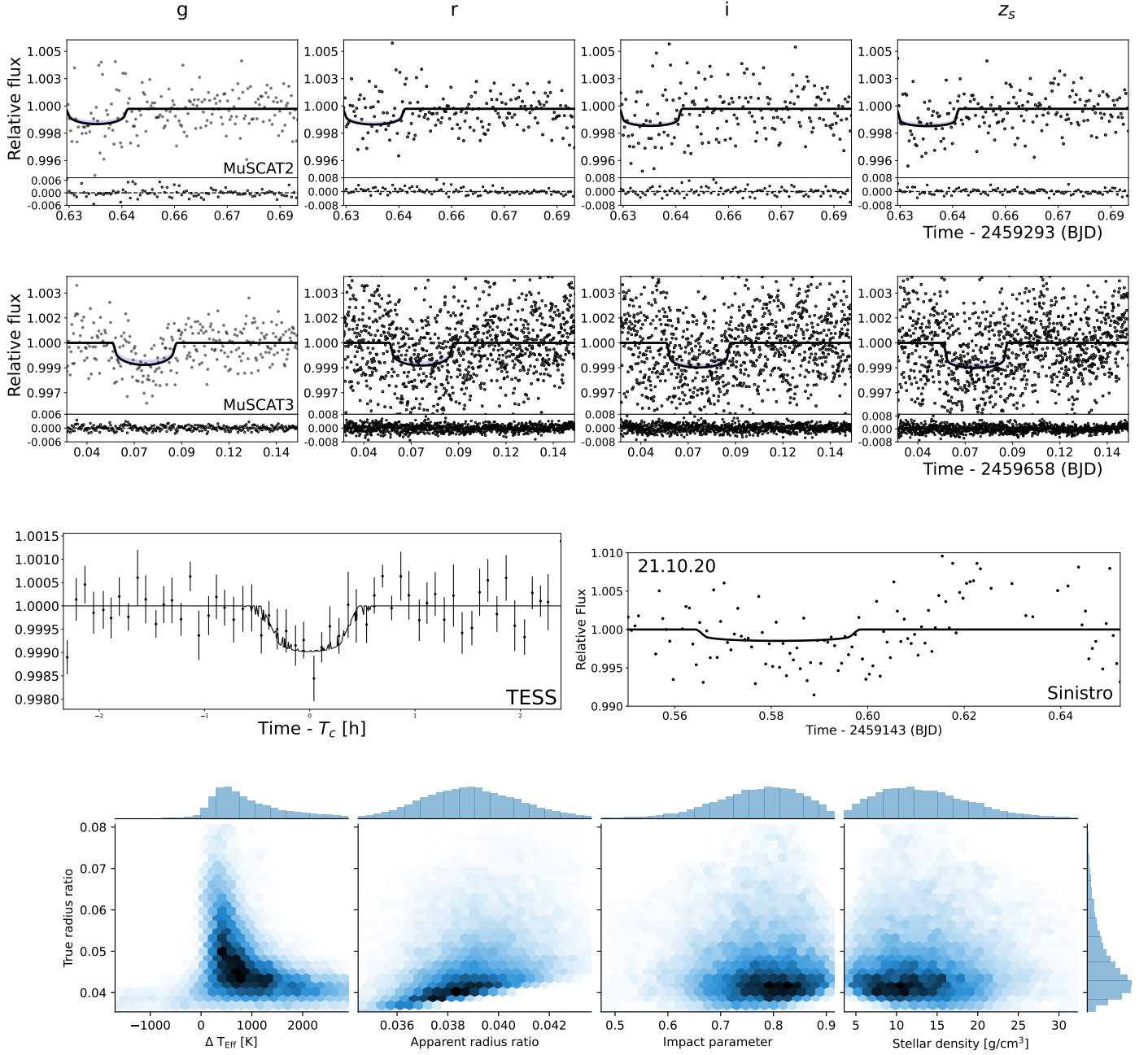


Fig. B.2. Same as Fig. B.1 for TOI-2274.01.

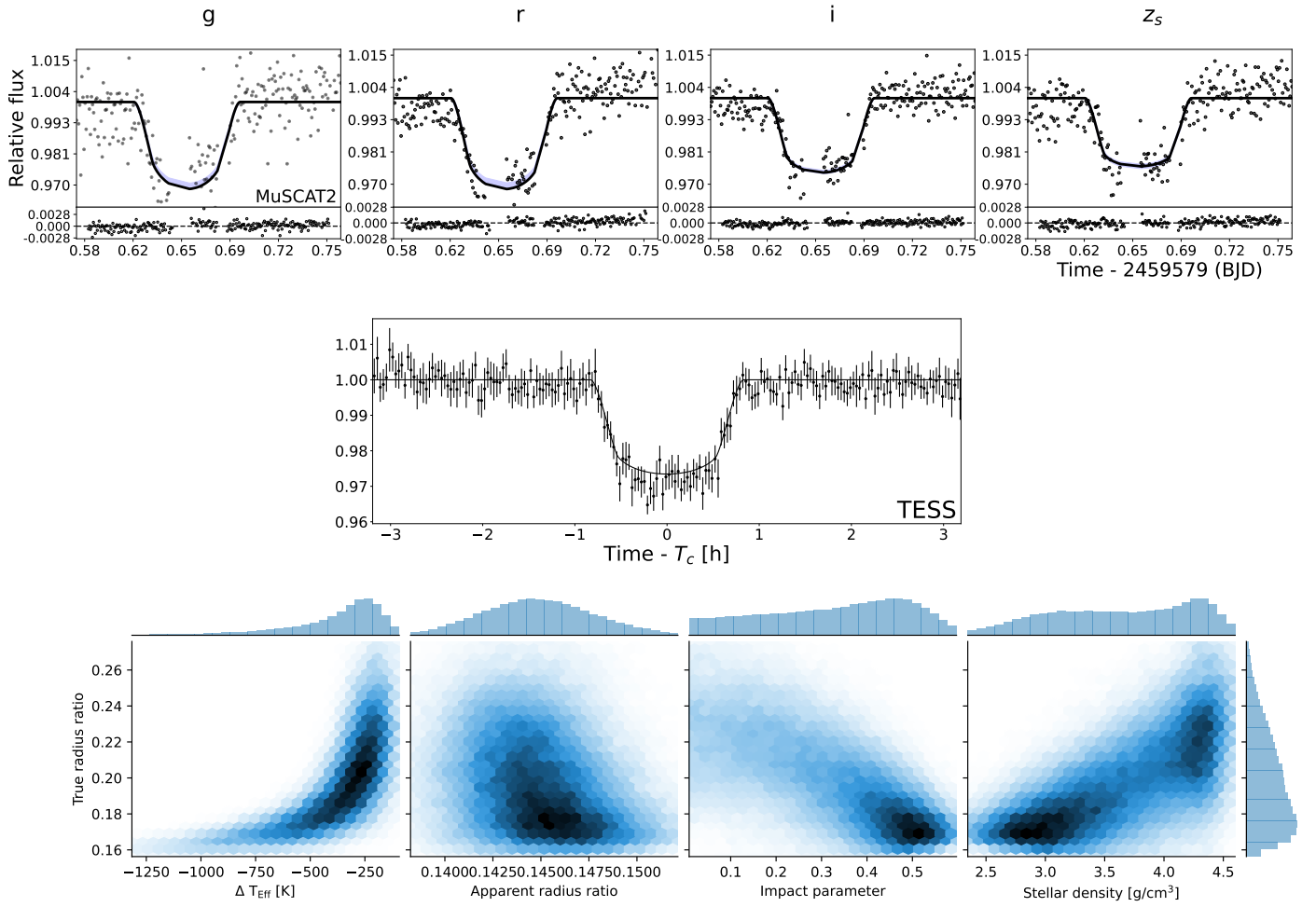


Fig. B.3. Same as Fig. B.1 for TOI-2603.01.

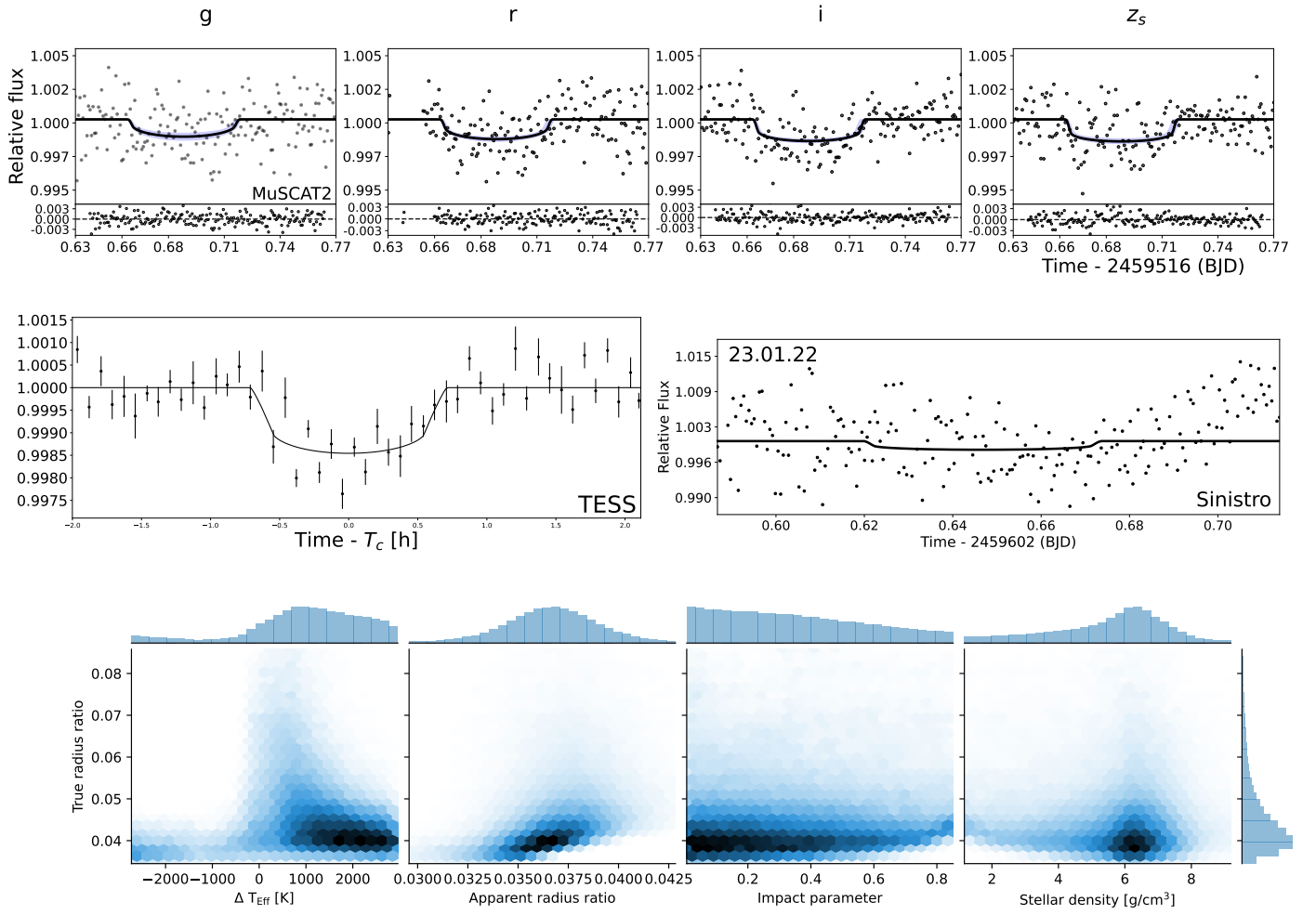


Fig. B.4. Same as Fig. B.1 for TOI-2768.01.

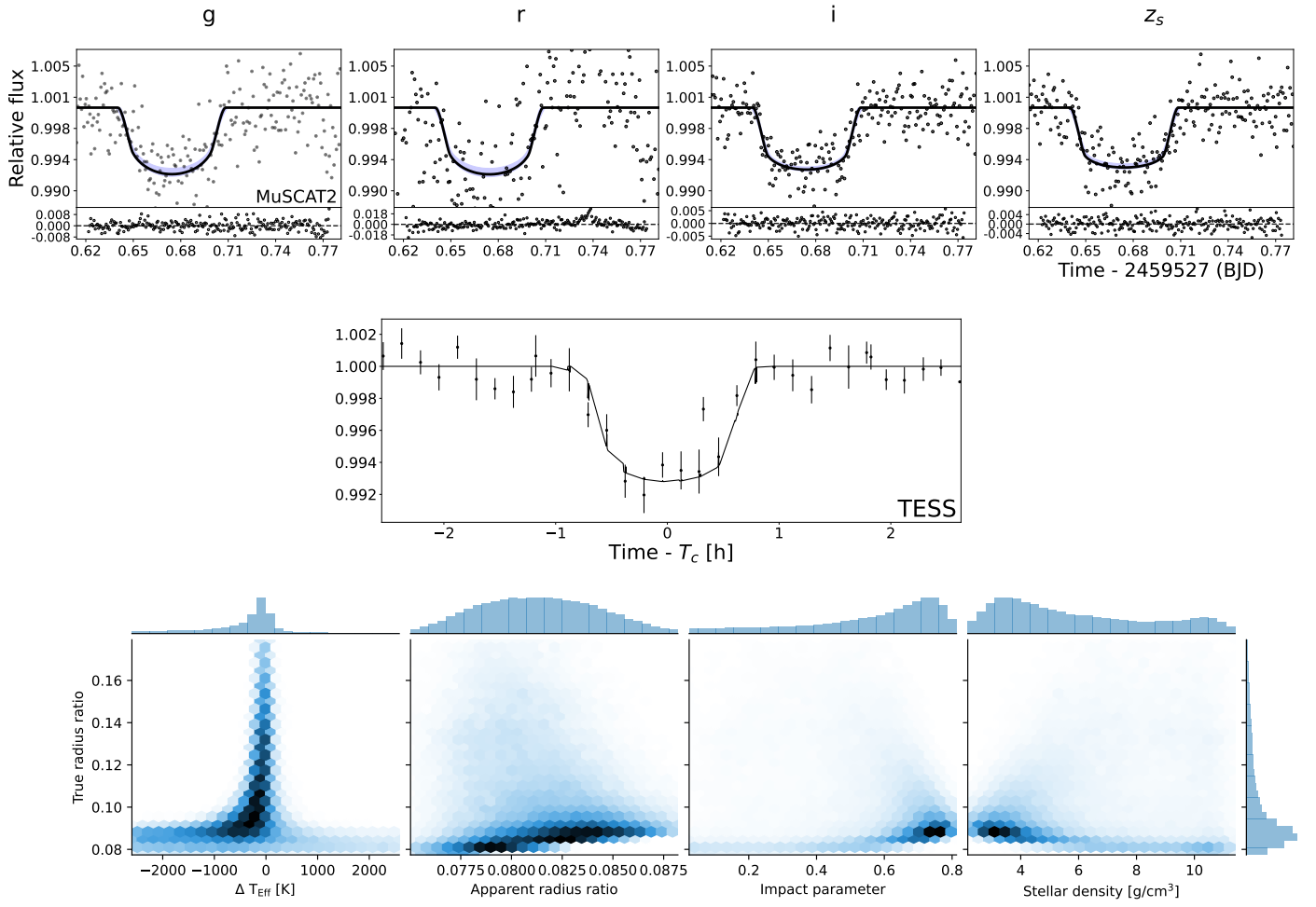


Fig. B.5. Same as Fig. B.1 for TOI-2781.01.

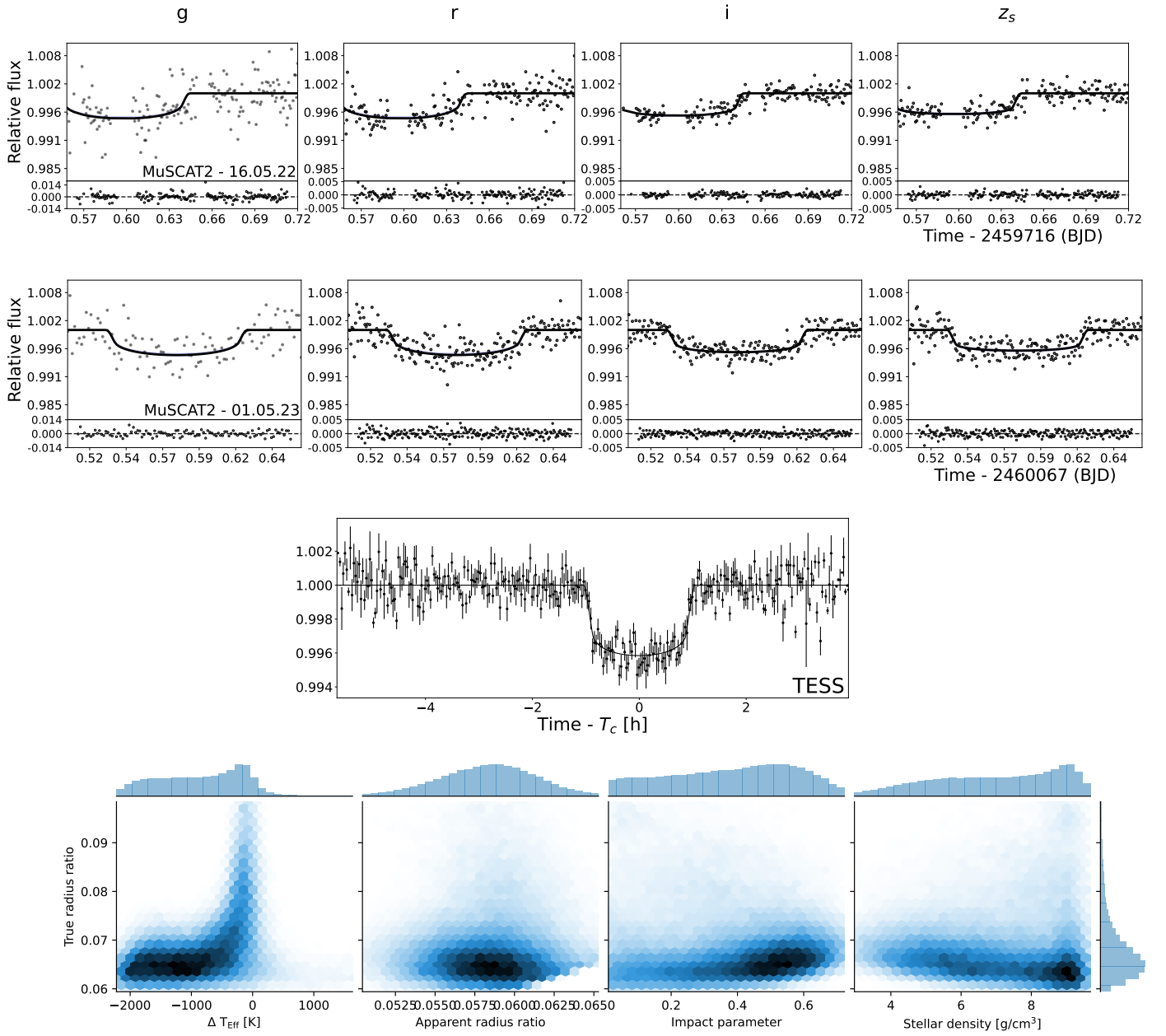


Fig. B.6. Same as Fig. B.1 for TOI-4438.01.

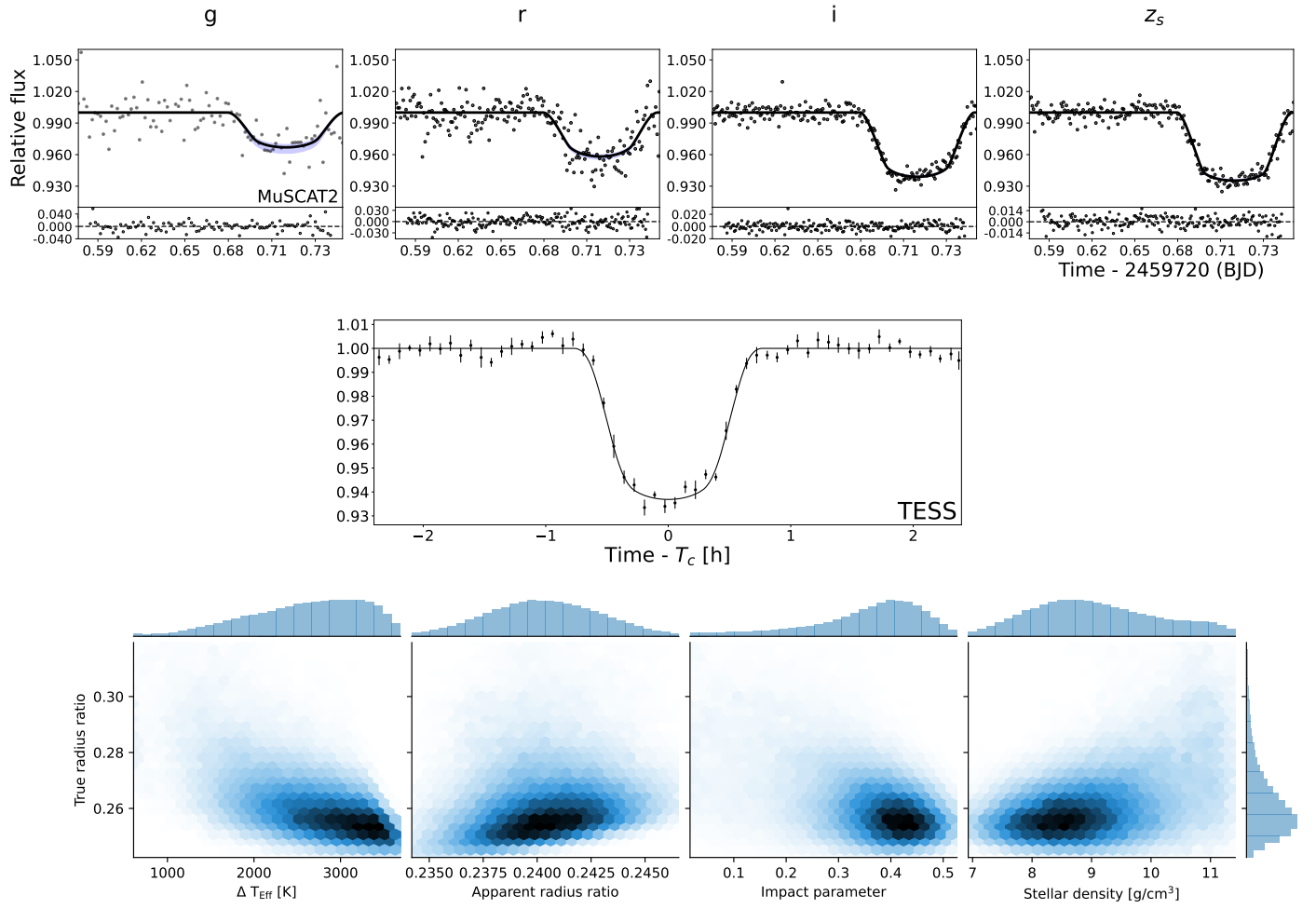


Fig. B.7. Same as Fig. B.1 for TOI-5205.01.

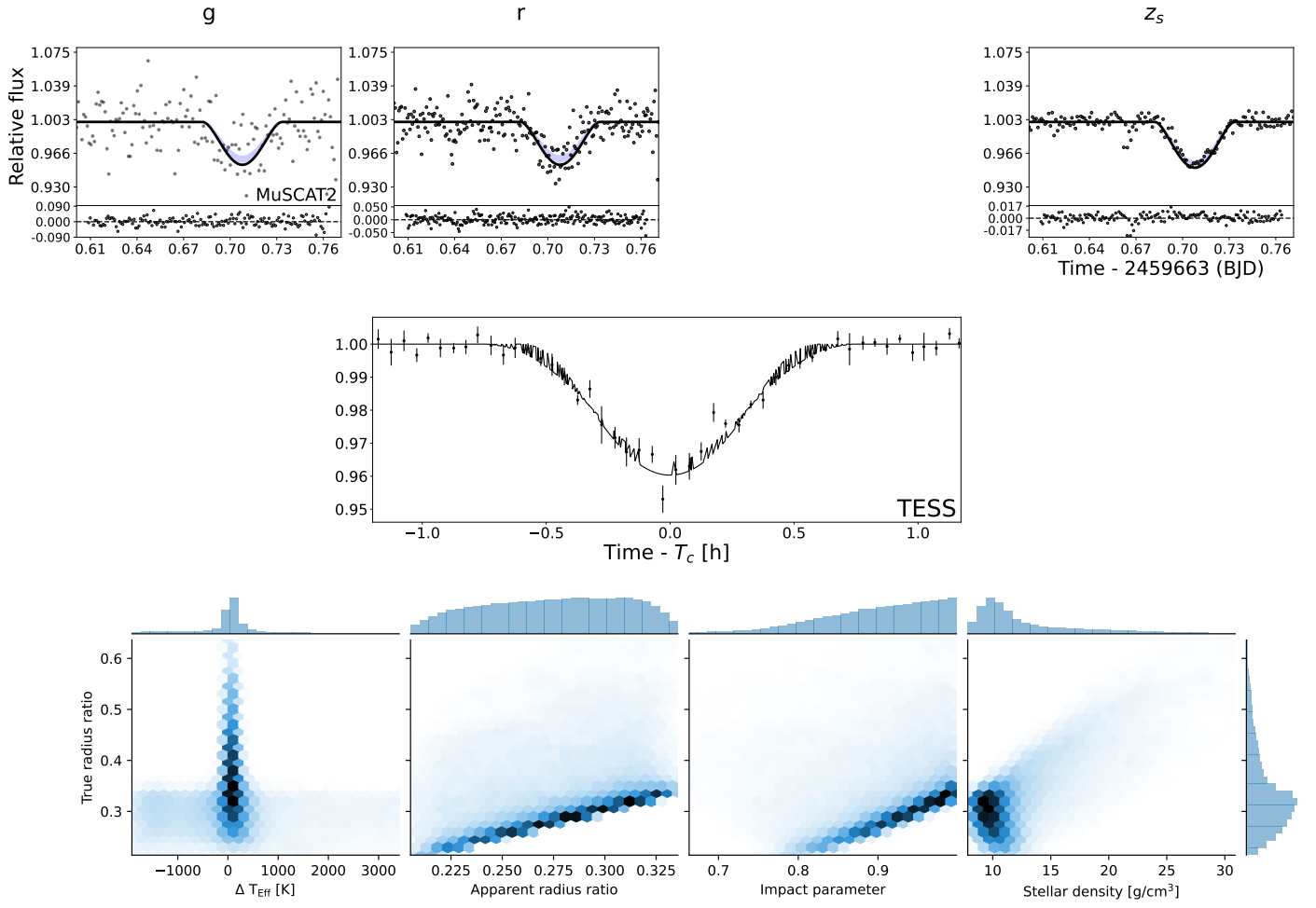


Fig. B.8. Same as Fig. B.1 for TOI-5268.01.

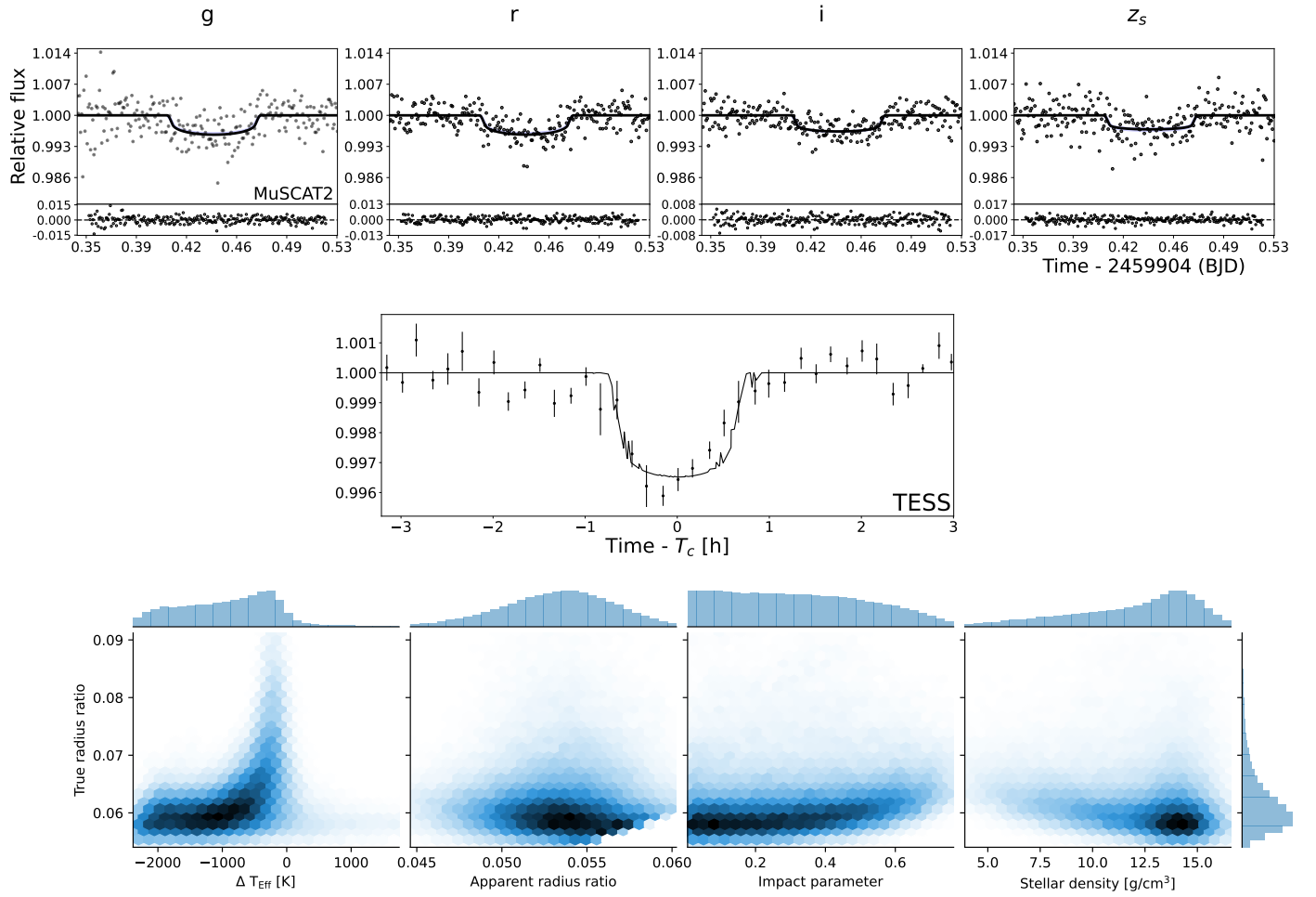


Fig. B.9. Same as Fig. B.1 for TOI-5319.01.

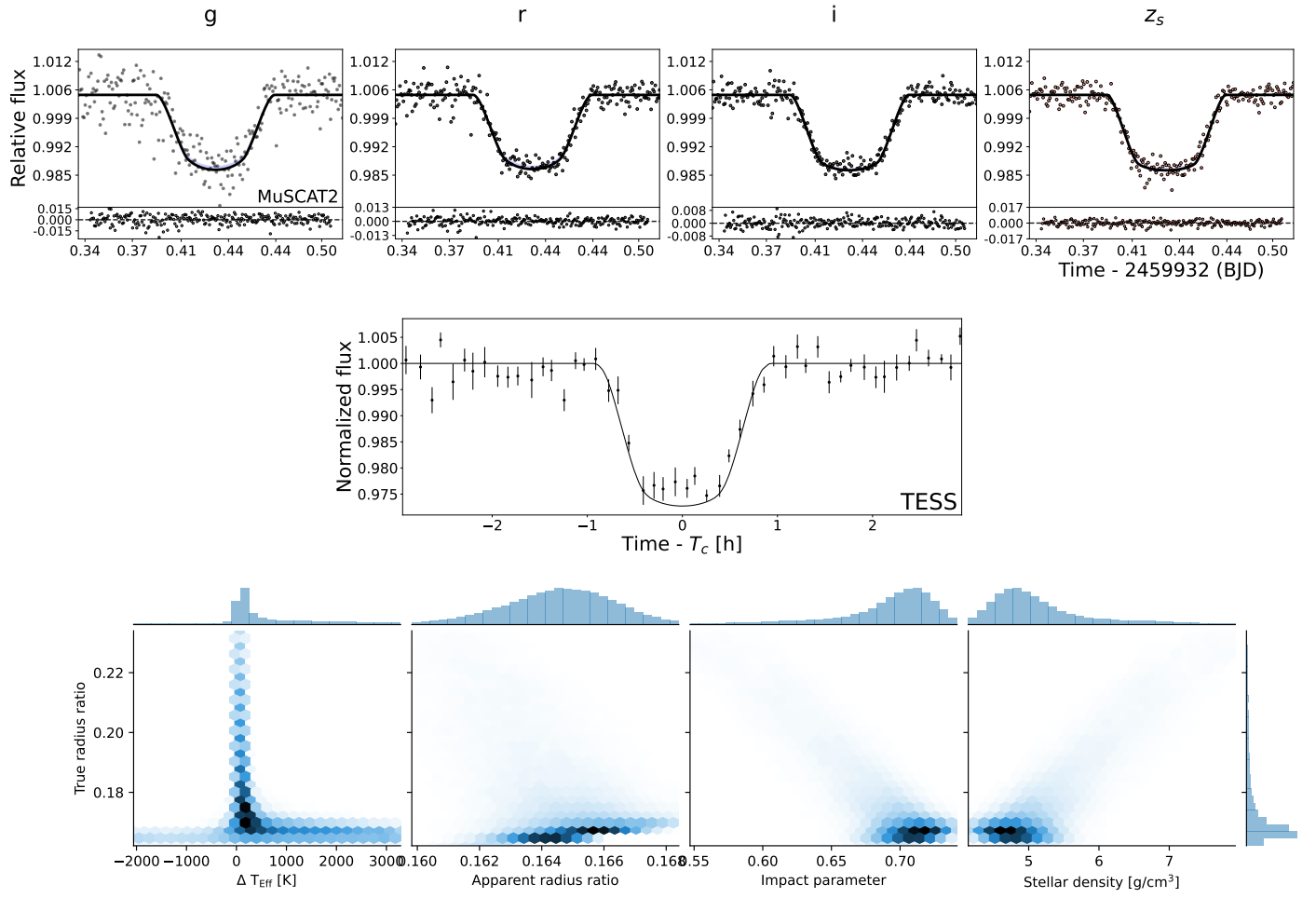


Fig. B.10. Same as Fig. B.1 for TOI-5344.01.

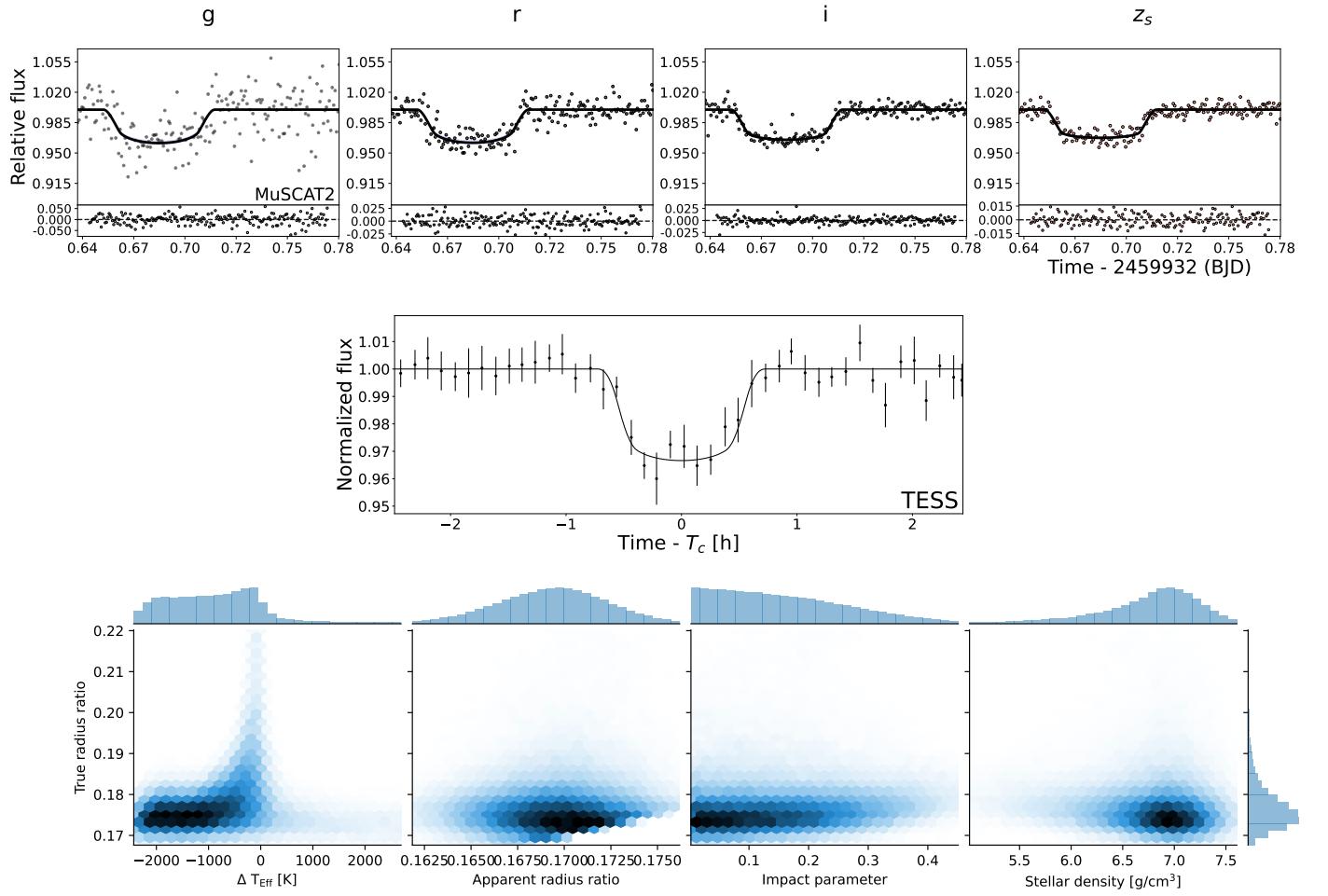


Fig. B.11. Same as Fig. B.1 for TOI-5464.01.

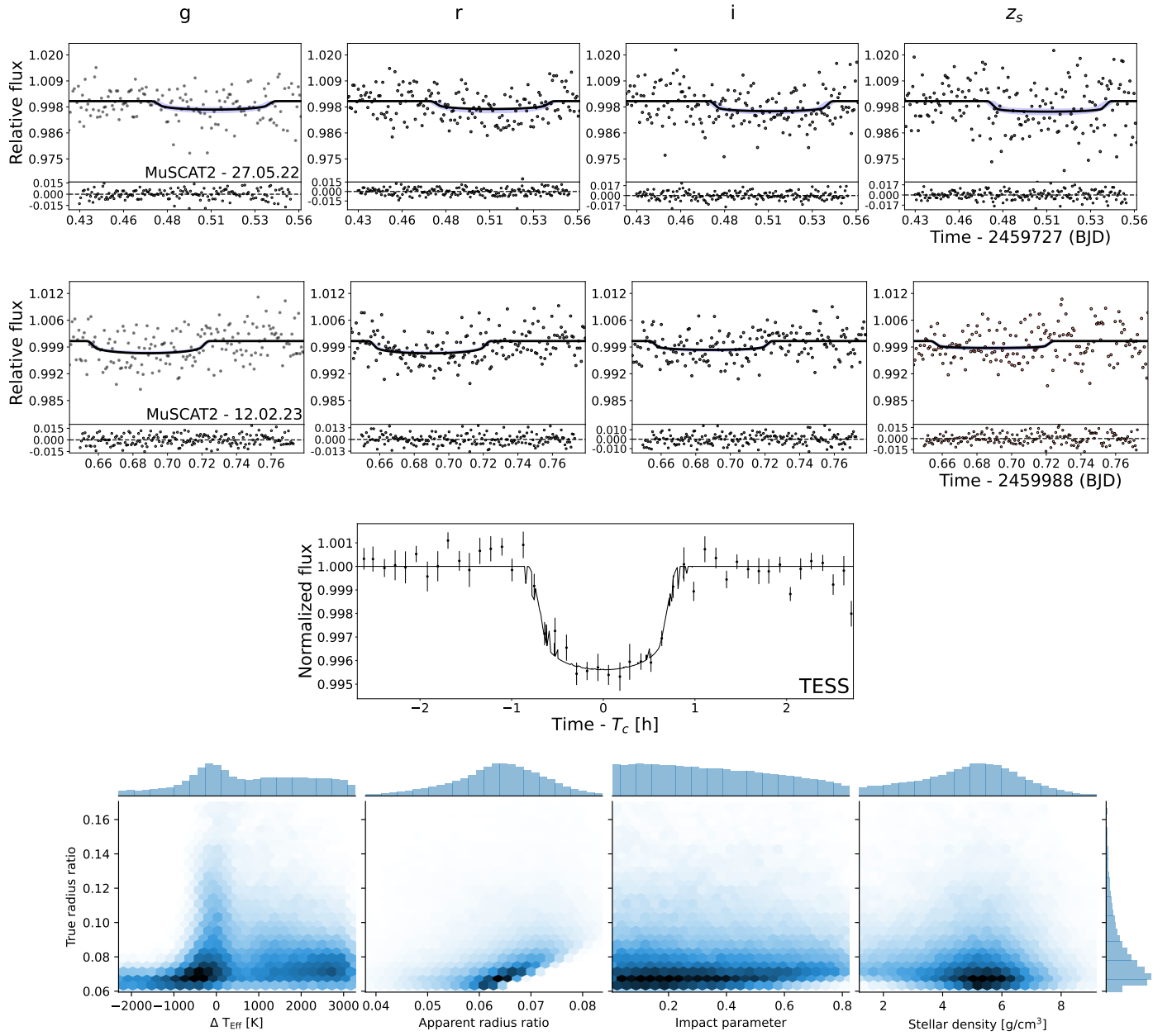


Fig. B.12. Same as Fig. B.1 for TOI-5486.

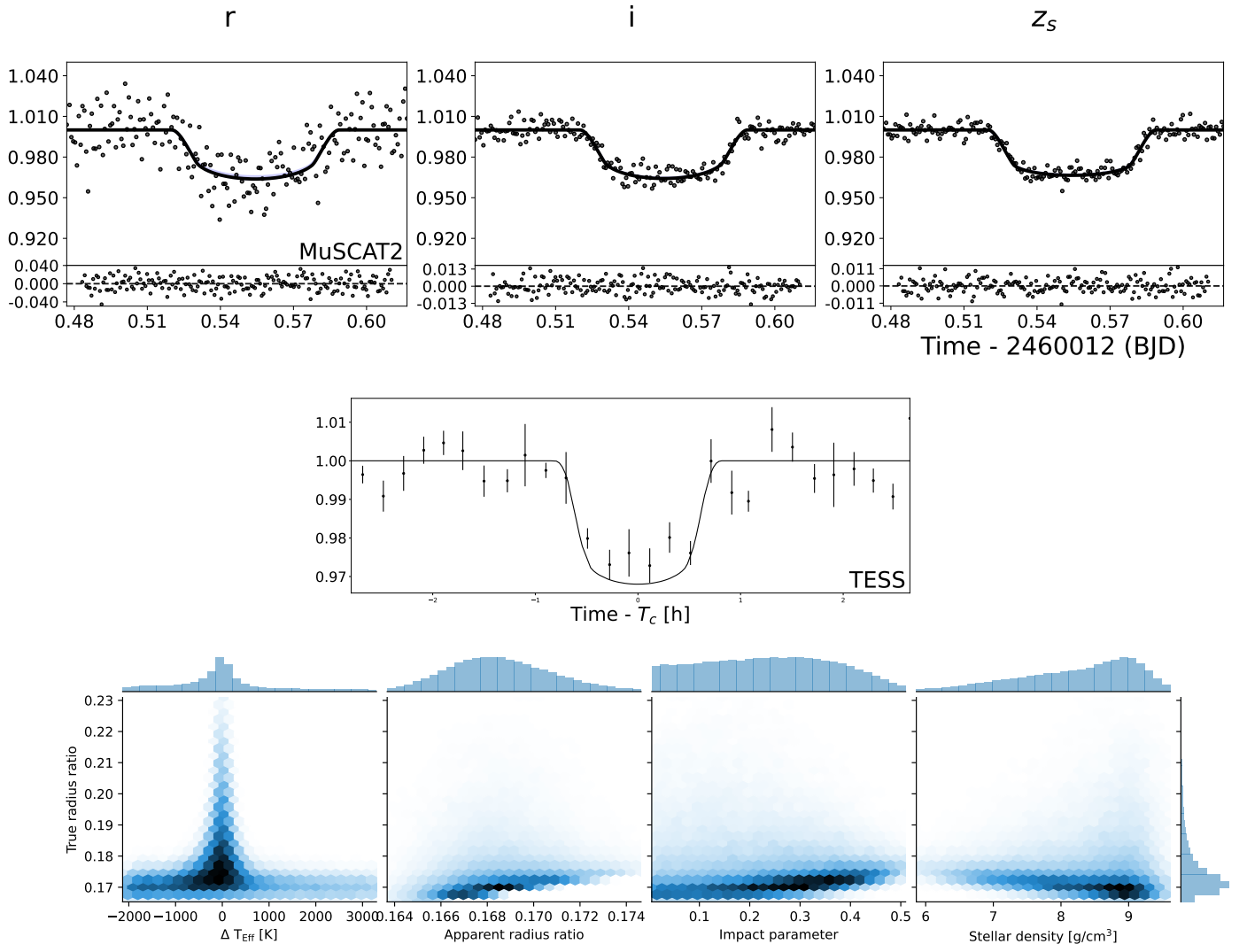


Fig. B.13. Same as Fig. B.1 for TOI-5641.01.

Appendix C: Stellar parameters

Table C.1. Stellar parameters for the stars hosting our candidates (ExoFOP 2019).

Main identifiers	TOI-1883	TOI-2274	TOI-2603	TOI-2768	TOI-2781	TOI-4438	TOI-5205-01
TIC	348755728	289164482	176772671	443556801	317417916	22233480	419411415
Equatorial Coordinates							
RA (J2000)	08:56:21.42	18:29:50.23	09:30:16	06:37:27.39	05:51:16.9	18:01:16.14	20:55:04.96
Dec (J2000)	-12:55:50.32	+40:32:29.08	-18:50:35.04	-15:28:52.33	-13:22:51.76	+35:35:41.64	+24:21:39.52
Parallax (mas)	8.51	20.46	4.26	12.79	6.20	33.26	11.46
Proper Motion RA ($\frac{mas}{year}$)	30.78	-14.87	-30.50	-82.63	-34.74	29.21	41.68
Proper Motion DEC ($\frac{mas}{year}$)	2.83	88.03	17.81	85.17	-24.36	-571.51	52.07
Magnitudes							
TESS	13.3462 \pm 0.0075	10.3543 \pm 0.0073	13.8995 \pm 0.0079	11.3676 \pm 0.006	12.9395 \pm 0.0073	11.2695 \pm 0.0073	13.6136 \pm 0.0089
V	15.792 \pm 0.069	11.995 \pm 0.063	15.529 \pm 0.297	12.66 \pm 0.069	14.525 \pm 0.149	13.69 \pm 0.045	15.899 \pm 1.03
<i>Gaia</i> DR2	14.5242 \pm 0.0005	11.2718 \pm 0.0008	14.8357 \pm 0.0016	12.2 \pm 0.0003	13.9312 \pm 0.0015	12.5196 \pm 0.0003	14.9317 \pm 0.0016
J	11.871 \pm 0.024	9.191 \pm 0.021	12.701 \pm 0.037	10.194 \pm 0.027	11.693 \pm 0.026	9.695 \pm 0.021	11.926 \pm 0.028
H	11.234 \pm 0.024	8.574 \pm 0.027	12.06 \pm 0.042	9.506 \pm 0.022	11.046 \pm 0.026	9.128 \pm 0.016	11.24 \pm 0.032
K	10.994 \pm 0.023	8.342 \pm 0.017	11.869 \pm 0.035	9.369 \pm 0.021	10.911 \pm 0.023	8.869 \pm 0.018	11.006 \pm 0.023
Stellar Parameters							
Spectral Type	M	M	M	M	M	M	M
$M_* [M_\odot]$	0.492 \pm 0.021	0.612 \pm 0.0202	0.584 \pm 0.023	0.63 \pm 0.079	0.662 \pm 0.022	0.364 \pm 0.0202	0.389 \pm 0.0204
$R_* [R_\odot]$	0.494 \pm 0.015	0.631 \pm 0.019	0.594 \pm 0.022	0.657 \pm 0.069	0.698 \pm 0.024	0.376 \pm 0.011	0.398 \pm 0.012
$L_* [L_\odot]$	0.03208 \pm 0.00778	0.08663 \pm 0.01896	0.07728 \pm 0.01817	0.10046 \pm 0.00836	0.09828 \pm 0.02292	0.016087 \pm 0.00399	0.01612 \pm 0.004103
$\log g [dex]$	≥ 4.5	≥ 4.5	≥ 4.5	≥ 4.5	≥ 4.5	≥ 4.5	≥ 4.5
$T_{eff} [K]$	3477 \pm 157	3943 \pm 157	3947 \pm 157	4008 \pm 130.393	3868 \pm 157	3353 \pm 157	3262 \pm 157
Distance [pc]	115.37 \pm 0.85	48.88 \pm 0.06		78.45 \pm 0.19		30.03 \pm 0.02	86.45 \pm 0.42

Table C.2. Same as Table C.1.

Main identifiers	TOI-5268	TOI-5319	TOI-5344	TOI-5464	TOI-5486	TOI-5641
TIC	202468443	246965431	16005254	171646471	291109653	141202786
Equatorial Coordinates						
RA (J2000)	15:16:01.48	02:20:51.25	04:13:03.89	10:35:06.07	12:42:11.88	12:03:38.2
Dec (J2000)	+62:43:05.73	+23:31:13.59	+20:54:54.56	+19:07:06.17	+03:47:18.96	+42:32:14.27
Parallax (mas)	10.27	16.45	7.31	3.55	11.09	5.22
Proper Motion RA ($\frac{mas}{year}$)	-9.66	42.12	40.42	-52.23	-59.78	-38.14
Proper Motion DEC ($\frac{mas}{year}$)	-20.21	-86.60	-22.19	21.96	-96.80	-70.73
Magnitudes						
TESS	14.5982 \pm 0.0074	12.0828 \pm 0.0061	13.2239 \pm 0.0074	14.9671 \pm 0.0084	12.2937 \pm 0.0072	14.5044 \pm 0.0075
V		13.947 \pm 0.018	15.402 \pm 0.149	17.24 \pm 0.2	14.297 \pm 0.059	17.06 \pm 0.2
<i>Gai</i> a DR2	15.9658 \pm 0.0009	13.1344 \pm 0.0008	14.3361 \pm 0.0006	16.0934 \pm 0.0021	13.3657 \pm 0.0002	15.7633 \pm 0.0013
J	12.818 \pm 0.021	10.35 \pm 0.028	11.799 \pm 0.021	13.569 \pm 0.022	10.983 \pm 0.024	12.991 \pm 0.023
H	12.218 \pm 0.023	9.7 \pm 0.028	11.087 \pm 0.022	12.964 \pm 0.025	10.342 \pm 0.024	12.43 \pm 0.021
K	11.965 \pm 0.022	9.553001 \pm 0.029	10.86 \pm 0.018	12.735 \pm 0.026	10.09 \pm 0.021	12.199 \pm 0.023
Stellar Parameters						
Spectral Type	M	M	M	M	M	M
$M_*/[M_\odot]$	0.285 \pm 0.0203	0.5 \pm 0.096	0.574 \pm 0.0204	0.525 \pm 0.022	0.548 \pm 0.0203	0.473933 \pm 0.0258296
$R_*/[R_\odot]$	0.307 \pm 0.009	0.485 \pm 0.067	0.583 \pm 0.018	0.528 \pm 0.018	0.553 \pm 0.0164	0.476 \pm 0.021
$L_*/[L_\odot]$	0.00850 \pm 0.00222	0.03475 \pm 0.00575	0.05009 \pm 0.01187451	0.0408144 \pm 0.009945498	0.04913394 \pm 0.01142	0.02662 \pm 0.00735
$\log g$ [dex]	≥ 4.5	≥ 4.5	≥ 4.5	≥ 4.5	≥ 4.5	≥ 4.5
T_{eff} [K]	3162 \pm 157	3580 \pm 124.253	3575 \pm 157	3572 \pm 157	3654 \pm 157	3379 \pm 157
Distance [pc]	97.08 \pm 0.60	61.17 \pm 0.21	138.37 \pm 1.32	282.85 \pm 5.84	89.68 \pm 0.27	215.996

Appendix D: Apparent-true radius ratio

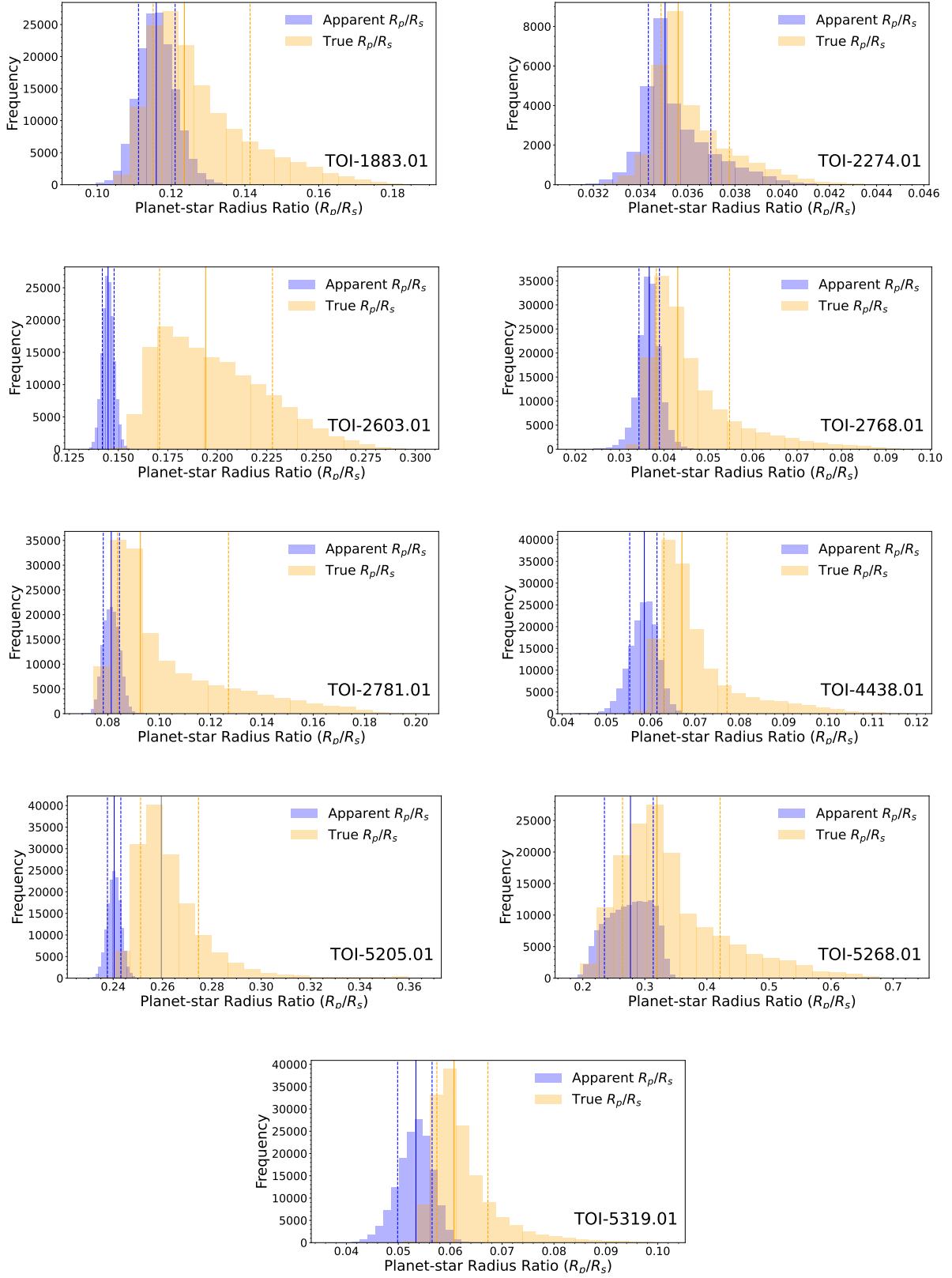


Fig. D.1. Apparent planetary radius (obtained straight from TESS achromatic data) in blue plotted over the true planetary radius (obtained from MuSCAT2 colored data) for all the candidates in the sample.

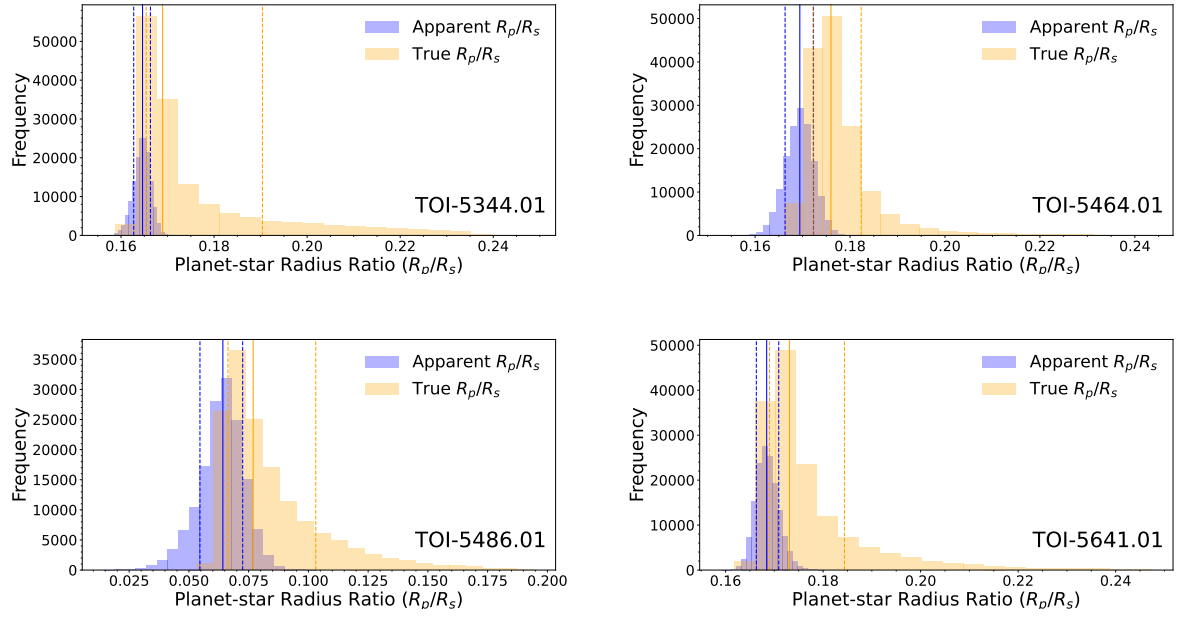


Fig. D.2. Same as Figure D.1.

Appendix E: Target pixel fields

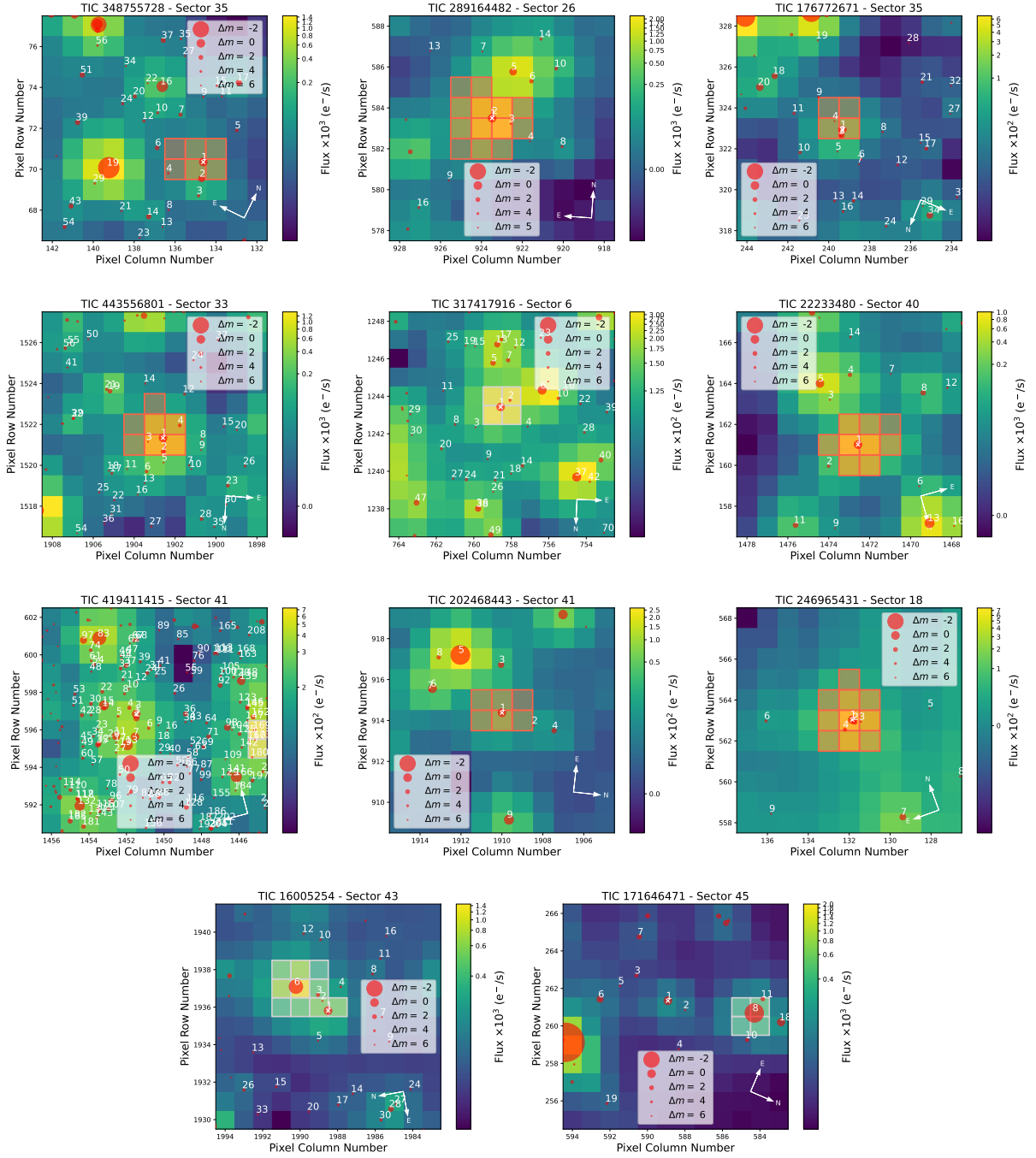


Fig. E.1. TESS target pixel file images for all the candidates among the sample observed in different sectors of the sky. The red circles show the sources in the field identified by the *Gaia* DR2 catalogue (Brown et al. 2018) with scaled magnitudes. The position of the targets are indicated by white crosses and the mosaic of orange squares show the mask used by the pipeline to extract photometry. These plots were made using *tpfplotter* (Aller et al. 2020).

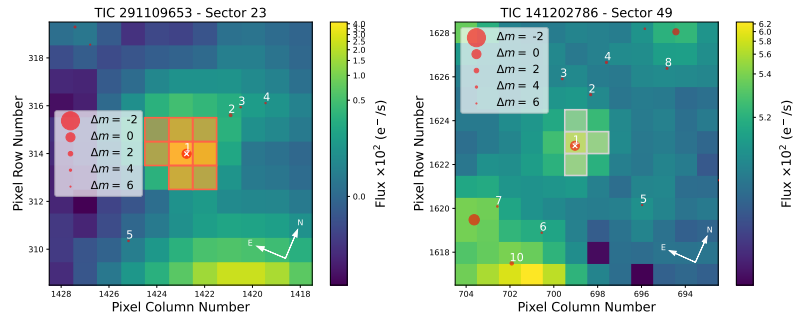


Fig. E.2. Same as Figure E.1.

Table E.1. On-sky distances and magnitudes of all blending stars inside the TESS mask of each target. Small numbers correspond to the star in the TPFs.

TOI ID	<i>Gaia</i> ID (blending stars)	G_{mag}	on-sky distances (arcsecs)
1883.01	² 5735743903992405632, ⁴ 5735743934056259456	15.19, 19.09	17.21946, 37.74068772454799
2274.01	² 2110345516767267328, ³ 2110322049065962624	15.63, 16.65	2.83068, 19.96109
2603.01	² 5678383069566114816, ³ 5678383069564973312, ⁴ 5678381592096224768	16, 18.73, 20.65	5.82608, 6.64550, 11.88246
2768.01	² 2950113808997899392, ³ 2950113808997903488, ⁴ 2950113602839471616	14.35, 17.89, 15.20	14.05505, 15.85573, 21.32742
2781.01	² 2996755813799995008	17.58	12.89655
4438.01	-		
5205.01	² 1842656663520848896, ³ 1842656663519264896, ⁴ 1842656659224186496	15.97, 20.45, 17.41	4.69377, 4.75093, 10.39776
5268.01	-		
5319.01	² 102461087706561280, ³ 102461083411745024, ⁴ 102461087706561408	14.58, 18.42, 15.76	3.38975, 9.15599, 12.63736
5344.01	² 52359538284125824, ³ 52359533989348224, ⁶ 52359744443457792	19.63, 16.89, 12.72	12.58189, 20.92206, 44.90926
5464.01	-		
5486.01	-		
5641.01	-		

Appendix F: Adaptive optic

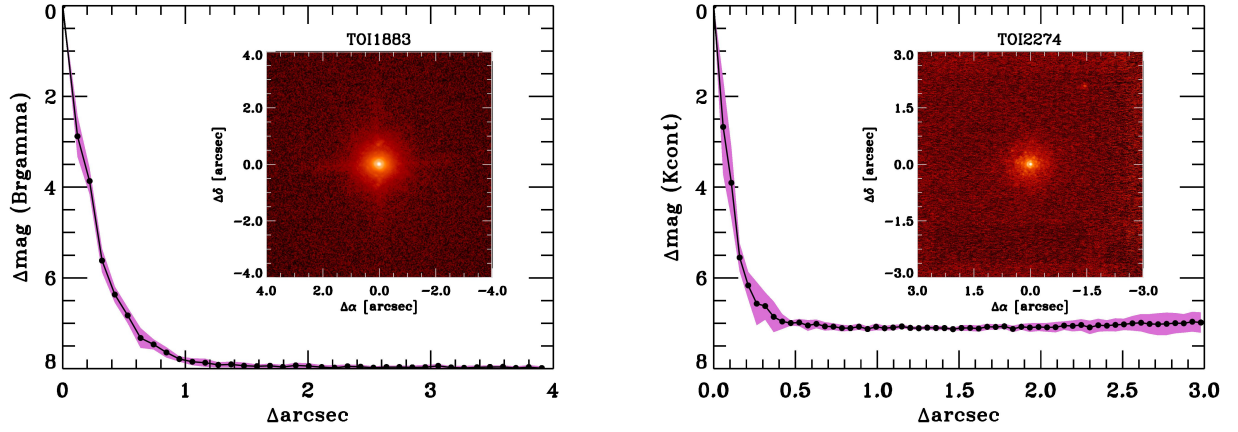


Fig. F.1. High-resolution imaging done by the NIRC2 instrument for TOI-1883.01 (left), and TOI-2274.01 (right).

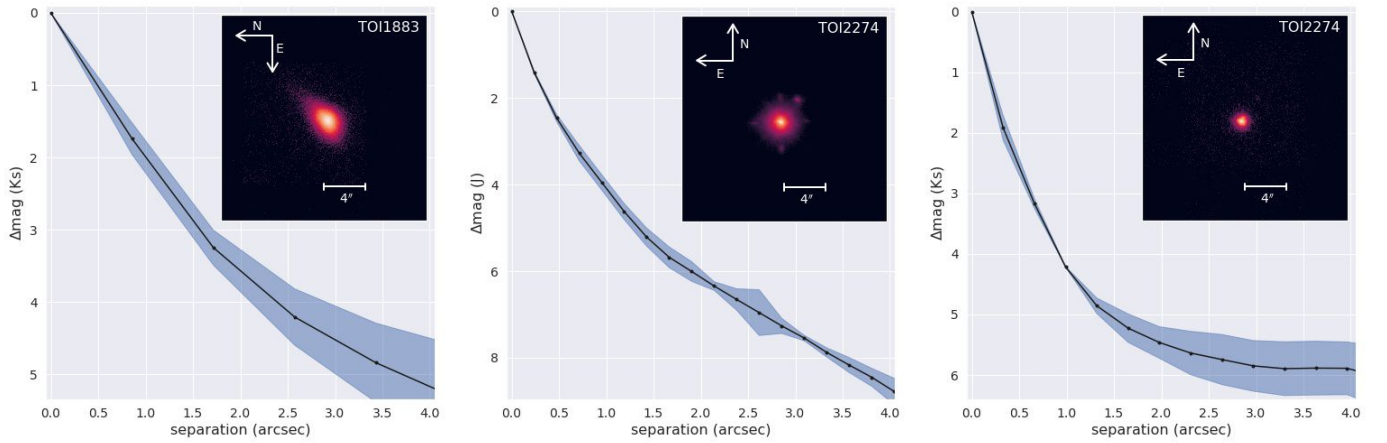


Fig. F.2. High-resolution imaging done by the shARCS instrument for both TOI-1883.01 and TOI-2274.01.

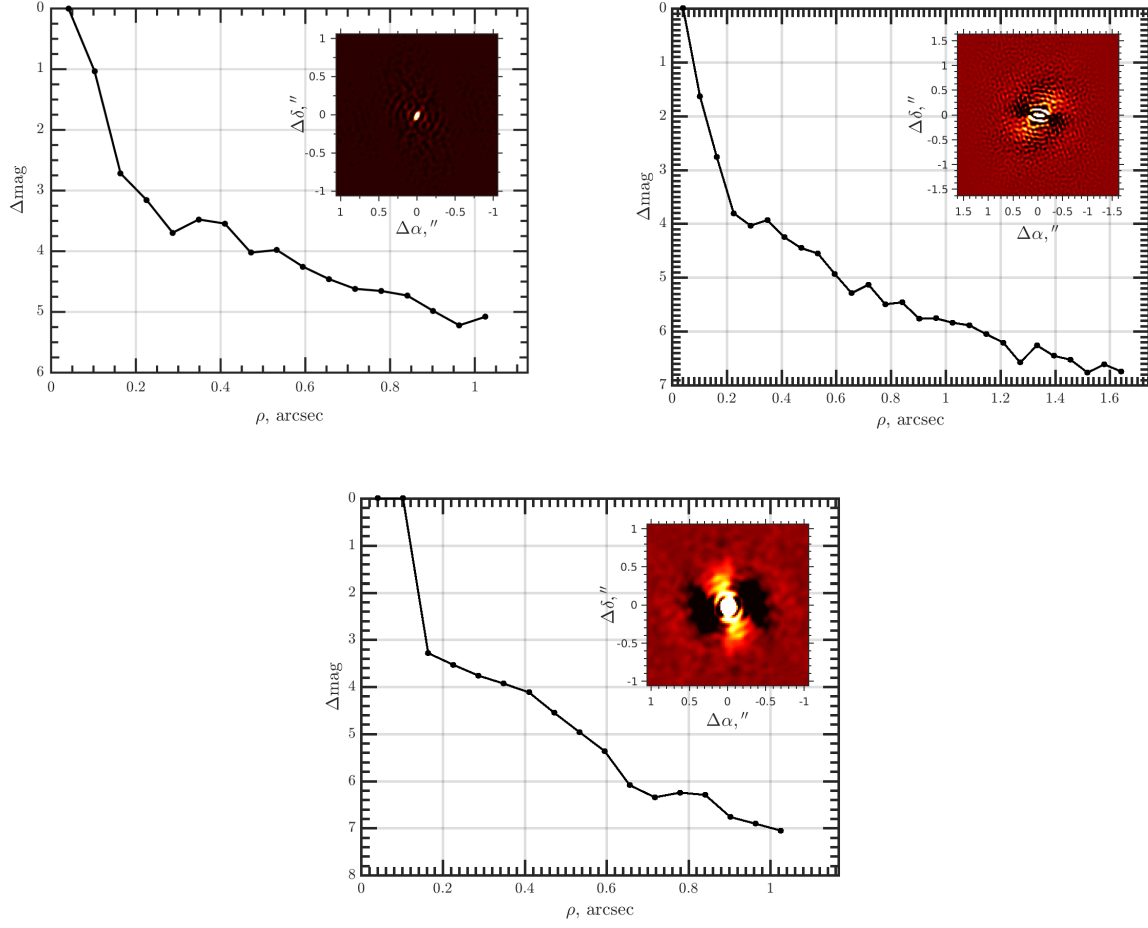


Fig. F.3. High-resolution imaging done by the Speckle Polarimeter instrument for TOI-2274.01, TOI-4438.01 and TOI-5319.01.

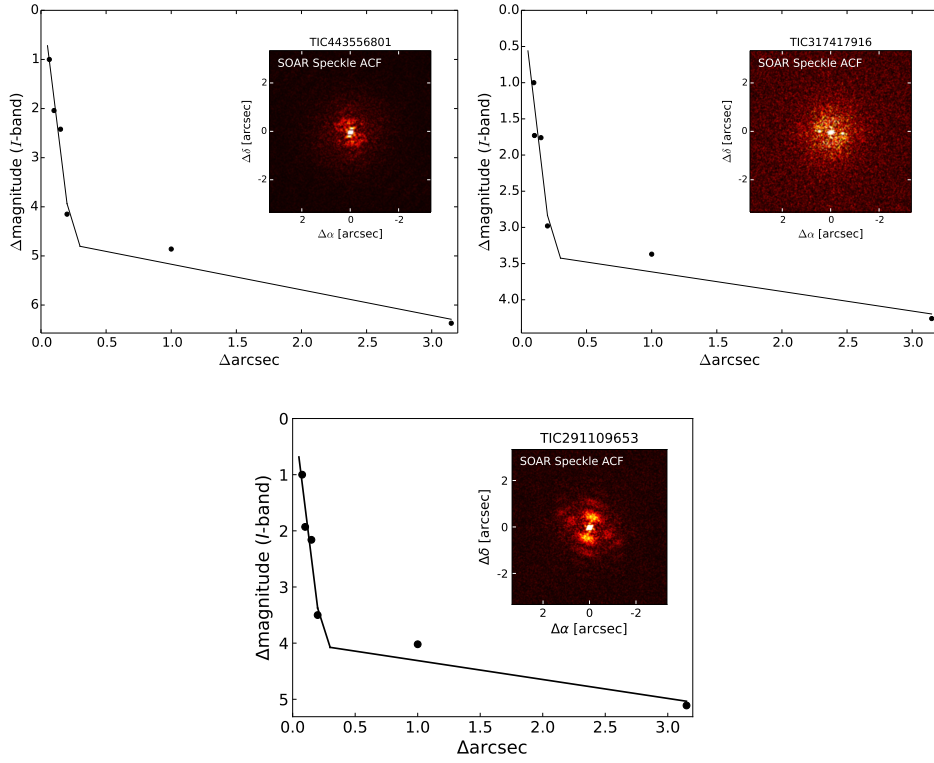


Fig. F.4. High-resolution imaging done by the HRCAM instrument for TOI-2768.01, TOI-2781.01, and TOI-5486.01.

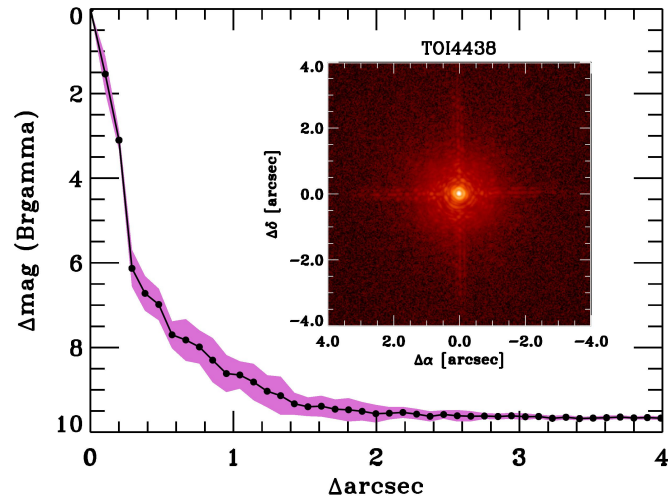


Fig. F.5. High-resolution imaging done by the PHARO instrument for TOI-4438.01.

Appendix G: Stellar spectra

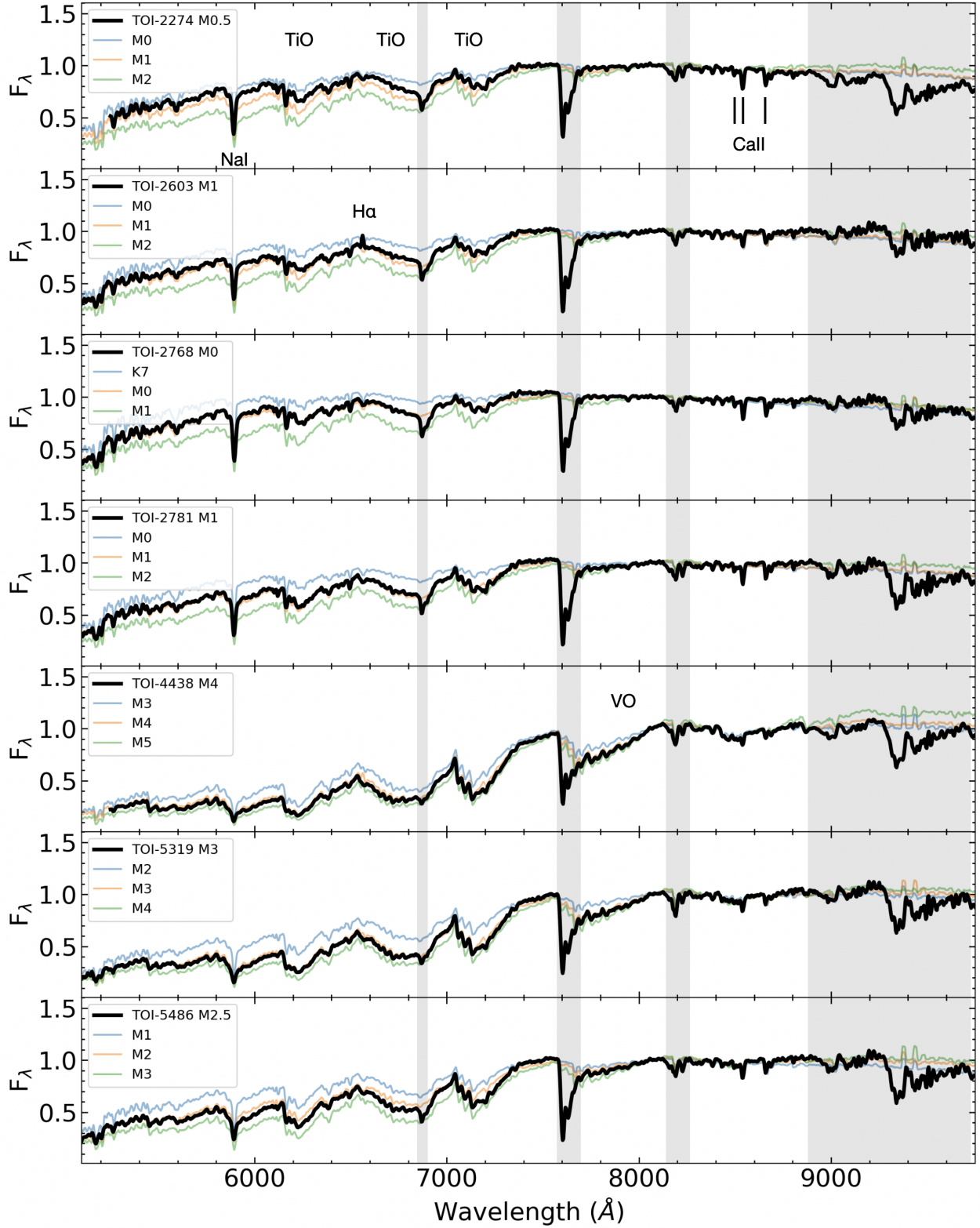


Fig. G.1. ALFOSC spectra of M dwarfs (thick black line) and various solar metallicity, spectral templates (colored lines) from the [Kesseli et al. \(2017\)](#) library. Strong telluric features are marked by the gray area. The strongest atomic and molecular features are labeled.